Inflamm. Res. (2012) 61:1299–1307
DOI 10.1007/s00011-012-0529-4

Inflammation Research

ORIGINAL RESEARCH PAPER

Liver X receptor activation attenuates plaque formation and improves vasomotor function of the aortic artery in atherosclerotic ApoE$^{-/-}$ mice

Jianghong Chen · Li Zhao · Dongdong Sun · Kazim Narsinh · Chunhong Li · Zheng Zhang · Shun Qi · Guangquan Wei · Weijie Li · Wenyi Guo · Feng Cao

Received: 14 February 2012 / Revised: 11 May 2012 / Accepted: 3 July 2012 / Published online: 26 July 2012

Abstract
Aim The severity of atherosclerosis is primarily determined by overall lipid metabolism and the degree of inflammation present within the vessel wall. We evaluated the effects of T-0901317, a liver X receptor agonist, on the atherosclerosis process, and especially on the endothelial function in ApoE$^{-/-}$ mice.
Methods and results ApoE$^{-/-}$ mice were treated with LXR agonist T-0901317 (1 μmol/L) for 6 weeks. ApoE$^{-/-}$ mice receiving T-0901317 were found to have markedly improved overall serum lipid profiles, albeit increased serum triglycerides. MRI imaging demonstrated that T-0901317 attenuated the atherosclerotic plaque burden in the aorta of ApoE$^{-/-}$ mice. Transmission electron microscopy and immunohistochemistry revealed attenuated ultrastructural changes as well as enhanced expression of the ATP-binding cassette transporter ABCA1. In addition, treatment with the LXR agonist improved the vasomotor function of atherosclerotic arteries, as assessed by KCl/norepinephrine-induced vasoconstrictive and acetylcholine-induced vasorelaxation functional assays. In vitro studies showed increased ABCG1, phospho-Akt and phospho-eNOS expression in ApoE$^{-/-}$ mice aorta endothelial cells (ECs) after T0901317 treatment.
Conclusion The present study suggest that LXR agonists protect the endothelium against atherosclerotic insults by increasing ABCA1 and ABCG1 expression, and improve the endothelial-dependent vasomotor function probably by promoting Akt and eNOS phosphorylation.

Keywords Liver X receptors (LXRs) · ATP-binding cassette transporter A1 (ABCA1) · Apolipoprotein E gene knockout (ApoE$^{-/-}$) mice · Atherosclerosis · Vasomotoricity · Endothelium

J. Chen, L. Zhao and D. Sun equally contributed to this work.

Responsible Editor: Ikuo Morita.

J. Chen · L. Zhao · D. Sun (✉) · C. Li · Z. Zhang · W. Li · W. Guo (✉) · F. Cao (✉)
Department of Cardiology, Xijing Hospital, Fourth Military Medical University, Xi'an 710032, Shaanxi, China
e-mail: wintersun3@gmail.com

W. Guo
e-mail: guowenyi@tom.com

F. Cao
e-mail: wind8828@gmail.com

S. Qi · G. Wei
Department of Radiology, Xijing Hospital, Fourth Military Medical University, Xi'an 710032, Shaanxi, China

K. Narsinh
Department of Radiology, Stanford Medical Center, Stanford University, Stanford, USA

Introduction

Atherosclerosis is a complex multifactorial condition in which dyslipidemia and inflammation play critical roles. Although lipid lowering agents such as HMG-CoA reductase inhibitors (Statins) retard the progression of atherosclerosis to some extent, their effects on plaque regression are generally modest. As a result, the investigation of new pharmacologic targets with the potential to modify atherosclerotic disease course remains an active and worthy endeavor.

Recently, liver X receptors have been identified as key regulating elements in lipid metabolism, with potential roles in the development of atherosclerosis. LXR agonists

have been previously shown to promote cholesterol efflux in macrophages, enhance synthesis of bile acid in the liver, and improve absorption of cholesterol in the gut [1]. Some synthetic LXR ligands have been developed, such as 22(*R*)-hydroxycholesterol, 24(*S*)-hydroxycholesterol (T0901317), GW3965 and *N*,*N*-dimethyl-3β-hydroxy-cholenamide (DMHCA). However, the effects of LXR agonists in vascular function and cardiovascular atherosclerosis have not been adequately clarified. The aims of our study were to investigate: (1) serum lipid profile, endothelium function, ultrastructural and immunohistochemistry changes of the aortic endothelium after administration with the LXR agonist T-0901317; (2) the possible mechanism of T-0901317 pretreatment.

Materials and methods

Animals and cells

Male ApoE$^{-/-}$ mice and C57BL/6 J mice at the age of 12 weeks (body weight 17–20 g) were provided by the Experimental Animal Center of Beijing University Medical College (Beijing, China) and the Experimental Animal Center of Fourth Military Medical University (Xi'an, China). The experiments were performed in adherence with the institutional guidelines on the use and care of laboratory animals.

Treatment groups

The animals were allocated to four groups ($n = 9$ in each group): (1) the control group (CON), C57BL/6 J mice with normal chow and treated with vehicle; (2) the LXR agonist treated control group (CON + LXRa), C57BL/6 J mice with normal chow and treated with LXR agonist T0901317 (Cayman); (3) the atherosclerosis model group (AS), ApoE$^{-/-}$ mice with high lipid chow and treated with vehicle; (4) the LXR agonist treated atherosclerosis group (AS + LXRa), ApoE$^{-/-}$ mice with high lipid chow and treated with T0901317. The high lipid chow was composed of 83.75 % normal chow, 1.25 % cholesterol and 15 % lard fat by weight. The T0901317 (10 mg/kg/day, dissolved with ethanol and diluted with water) was intragastrically administered everyday between 9 to 11 a.m. for 6 weeks, and blood and tissue samples were collected for further examination.

Aortic endothelial cells were isolated and cultured from 12-week old ApoE$^{-/-}$ mice. Briefly, the full length of the thoracic aorta was removed under sterile conditions, rinsed 3 times with PBS, and placed into a 100-mm culture dish filled with serum-free culture medium on ice. The vessel was gently cleaned of periadventitial fat and connective tissue, cut to expose the luminal surface, and rinsed with the culture medium. The surface was then covered with a collagenase solution (II and IV, 1 mg/mL), and incubated at 37 °C for 1 h. After incubation, the solution containing detached endothelial cells was aspirated and placed in a tube with 5 mL medium plus serum to arrest the digestion process. The vessel surface was then subjected to a forceful stream of the culture medium using a 10-mL syringe to collect the remaining cells loosely attached to the surface. Finally, the vessel was rinsed with the medium, and the medium containing additional cells was collected and combined with the initial aspirate. The cell suspension was centrifuged at 2000 rpm for 10 min. The cell pellet was washed twice, suspended in medium to a total volume of 2 mL, and placed in a 60-mm culture dish. The dish was then placed in a humidified incubator at 37 °C with 5 % CO_2. After 2 days, 2 mL of fresh medium was added to the dish, and the incubation was continued for an additional 2 days. The medium was changed every other day.

ECs were further subjected to vehicle (group A) or T0901317 (1 μmol/L, group B) treatment for 1 h alone, or followed by cholesterol (25 ug/ml) stimulation (vehicle plus cholesterol, group C; T0901317 plus cholesterol, group D) for 24 h. In an attempt to explore the mechanisms of T0901317 effects, the phosphotidylinositol 3-kinase (PI3 K) inhibitor LY294002 was added for an additional hour in a separate group (T0901317 plus LY294002, group E). The cells were harvested at the end of treatment and processed for western blot analysis.

Blood serum cholesterol determination

Blood samples were collected from the orbital veins, and the serum was separated after blood coagulation. The serum levels of triglycerides (TG), total cholesterol (TC), low-density lipoprotein cholesterol (LDL-C) and high-density lipoprotein cholesterol (HDL-C) were measured by an automatic biochemical processer (Olympus Au2700).

MRI imaging of the aortic wall

All MRI scans were performed on a 3.0 T MR scanner (MAGNETOM Trio, Siemens AG, Erlangen, Germany). Mice were initially anesthetized with 4 % isoflurane in oxygen (0.4 L/min) and placed head-up in a 40 mm bird-cage coil for imaging (Siemens). During MRI, anesthesia was maintained using 1.5–2.0 % isoflurane in oxygen (0.4 L/min) supplied through a face mask. The respiratory signal was monitored using a pressure sensor to regulate the depth of the anesthesia.

Gradient-echo coronal images were used to localize the thoracic and abdominal aorta. Thereafter, sequential axial images of the aorta from the arch to the iliac bifurcation

were obtained using trueFISP (true fast imaging with steady state) sequence with the following parameters: TR = 35 ms, TE = 1.2 ms, matrix = 256 × 256, FOV = 2.6 × 2.6 cm^2, and slice thickness = 0.58 mm, GRAPPA factor = 2, flip angle = 65°, NEX = 12.

Transmission electron microscopy observation of the aortic wall

The ultrastructure of the aortic wall was investigated by transmission electron microscopy. Briefly, the thoracic aortic segments were pre-fixed with 3 % glutaraldehyde for 2 h, dipped into 10 mmol/L phosphate buffered saline (PBS) for 3 times (10 min each), and post-fixed with 1 % osmic acid for 30 min. The samples were then rinsed with PBS, dehydrated, embedded with Epon 812 epoxide resin, and sliced with the LKB-Nova into ultra-thin slices (20 nm thickness). After staining with uranium salt and lead salt, the slices were observed under JEM-2000SX transmission electron microscope (JEOL Ltd, Japan).

Measurement of isometric force

In vitro measurement of isometric force was performed as described by Zhang et al. [2] and Sangha et al [3]. Briefly, thoracic aortic rings (3 mm in length at the para-root segments) were isolated and mounted horizontally on two stainless steel hooks and placed on stainless steel holders in tissue baths (isolated tissue bath, Radnoti) for vasoreactivity recordings with PowerLab (AD Instruments). The bathing chamber contained 8 ml of Krebs buffer solution maintained at 37 °C and bubbled continuously with 95 % O_2–5 % CO_2. Individual arteries were allowed to equilibrate for 60 min and then loaded to optimal resting tension. After loading, arteries were washed with Krebs buffer every 10 min in the myograph bath and left to equilibrate until they were at a steady baseline. After the artery mounting and preparations were concluded, arteries were challenged with KCl (0–100 mM), cumulative concentrations (10^{-10}–10^{-4} mol/L) of phenylephrine (PE). KCl (60 mM) was used to induce arterial contraction, which was then relaxed by acetylcholine (ACh 10^{-10}–10^{-4} mol/L) and sodium nitroprusside (SNP 10^{-10}–10^{-4} mol/L), respectively. Cumulative concentration–response curves were generated. Vasodilatation was represented as the percentage of maximal contraction to KCl at 60 mM. Fifty percent effective concentration (EC50) was used to evaluate sensitivity to vasoactive substances in the present study.

Histological analysis

The thoracic aorta samples were stained with routine H and E as well as immunohistochemically with the ABCA1 antibody. Briefly, the samples were harvested, washed with PBS, fixed with 4 % paraformaldehyde and cryo-sliced. The slices were inactivated with 30 % H_2O_2–methanol for 30 min, permeabilized with 0.3 % Triton X-100 in PBS for 30 min, and incubated with rabbit polyclonal antibody against ABCA1 (1:200 dilated, Abcam) overnight at 4 °C. After washing 3 times, a goat anti-rabbit secondary antibody (1:400, Santa Cruz) was added and incubated for 2 h at room temperature. The HRP-DAB reagent (Roche diagnostics, Mannheim, Germany) was then added to the slice and incubated for 60 min. A DAB visualization kit (Biostar, Wuhan, China) was used to visualize the staining. The slice was then dehydrated, mounted, and microscopically examined. Atherosclerosis was analyzed blindly in four cross-sections of each specimen (at intervals of 40 μm). The luminal area and the area bounded by the internal elastic laminae were measured on each arterial cross-section using the Image-Pro Plus software (Media Cybernetics) and served to compute intimal area. The density of ABCA1 signal of the intima was measured digitally using an automated, contrast-based, area analysis function of the Image-Pro Plus software.

Western blot analysis

Full length aortic tissues and EC cell pellets were homogenized in ice-cold homogenization buffer (Beyotime, China), using a glass/glass homogenizer. The homogenate was centrifuged at 3,000 g for 5 min to remove insoluble material. Protein concentration was determined (BCA assay, Pierce, USA), and 10 μg of protein extract from each sample were subjected to 8 % SDS-PAGE and electro-transferred onto PVDF membrane. Membranes were blocked with 5 % skim milk and 0.1 % Tween 20 for 1 h at room temperature and then incubated with rabbit polyclonal antibodies against ABCA1 (Abcam, USA), ABCG1 (Abcam, USA), phospho-Akt (Ser473) (Cell Signaling, USA) or phospho-eNOS (Ser1177) (Cell Signaling, USA) at 4 °C overnight. The membranes were then washed and incubated with the secondary antibody (HRP-labeled anti-rabbit IgG, Santa Cruz) at 37 °C for 60 min. Reactions with antibodies were visualized using a chemiluminescence kit (Beyotime, China) and Hyperfilm ECL (Amersham, USA).

Statistical analysis

Results are presented as mean ± SD. All results were analyzed with GraphPad Prism 5.0 software. Comparisons among groups were performed by one way ANOVA, followed by LSD t test for post hoc analysis. A probability value of <0.05 was considered statistically significant.

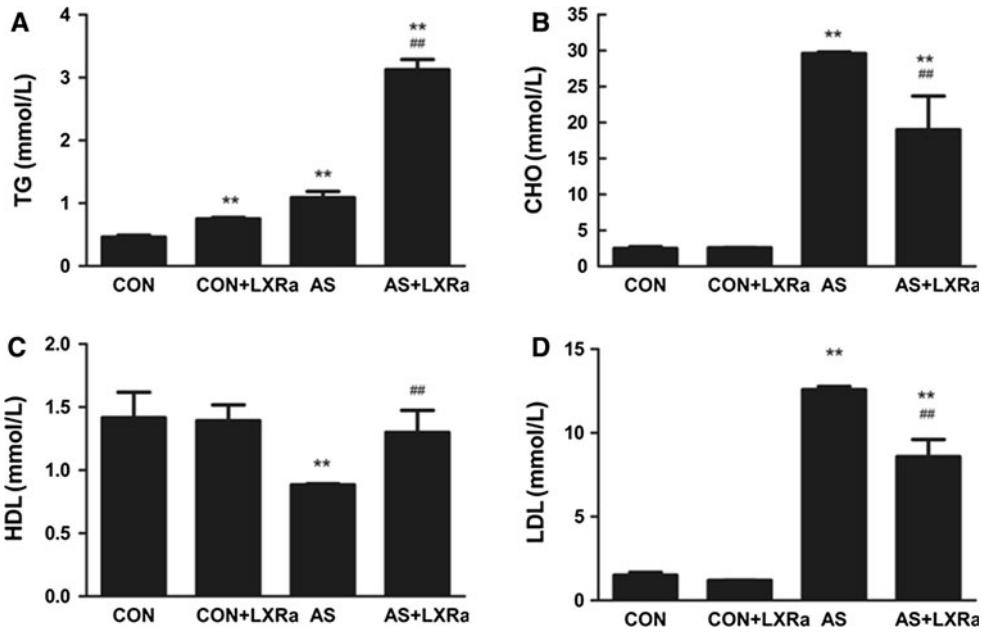

Fig. 1 Lipid profiles of control and T0901317-treated, regular chow or cholesterol-fed ApoE$^{-/-}$ mice. Shown are the serum lipid profiles measured of the four experimental groups ($n = 6$ for each group) at the end of the 6-week treatment period. **a** Triglycerides content in serum samples. **b** Total cholesterol content in serum samples. **c** High density lipoprotein level in serum samples. **d** Low density lipoprotein level in serum samples. Data represent mean values ± SEM. $^{**}P < 0.05$ vs. CON (control) group, $^{\#\#}P < 0.05$ vs. AS (atherosclerosis) group

Results

T-0901317 pretreatment decreased the serum lipid profile

After 16 weeks of feeding, there was no significant difference in body weight between the four groups. High serum levels of LDL-C, CHO, and TG were confirmed in the atherosclerotic model (Fig. 1a, b, d). The LDL-C level of the AS and AS + LXRa groups was significantly elevated compared to the CON and CON + LXRa groups (all $P < 0.05$). The AS + LXRa treatment group had higher serum levels of HDL-C and TG ($P < 0.05$) but lower levels of TC and LDL-C ($P < 0.05$) compared to the untreated AS model group (Fig. 1c), consistent with previous reports [4].

T-0901317 attenuated the atherosclerotic plaques burden

MRI imaging demonstrated that there were diffuse atherosclerotic plaques in the aorta of ApoE$^{-/-}$ mice (AS group) (Fig. 2a). The AS + LXRa group showed decreased atherosclerotic plaques burden and clear vessel wall structure of the aorta as compared with the AS group (Fig. 2b).

T-0901317 decreased the severity of atherosclerosis

Immunohistochemical staining demonstrated ABCA1 expression principally around the aortic endothelium. The AS + LXRa group showed a 54.9 % reduction of intimal area compared with the AS group (Fig. 3f, h, i, $P < 0.05$). Endothelial ABCA1 staining was markedly elevated in the AS group as well as in the AS + LXRa group (Fig. 3a, c, e, g, j). ABCA1 signal had a slight tendency toward increase in the AS + LXRa group (Fig. 3g) as compared to the AS group (Fig. 3e, 9.5 %, not significant).

T-0901317 pretreatment attenuated the ultrastructure changes of the aortic wall

We next sought to examine the ultrastructure changes of para-root aortic sections using electron microscopy. The CON and CON + LXRa groups showed intact endothelium and clear vessel wall structure (Fig. 4a, b). However, in the AS group, extensive thickening and fibrosis of the intima as well as detachment of the endothelium were observed. Other hallmarks of atherosclerosis, including ample foam cells (black arrow), migrant smooth muscle cells (red arrow), and cholesterol crystals (yellow arrow) were observed in the AS group (Fig. 4c). The AS + LXRa treatment group retained some features of atherosclerosis, such as an unclear vessel wall structure and a thickened intima. However, the number of foam cells, migrating smooth muscle cells and cholesterol crystals were obviously less than in the untreated AS group (Fig. 4d).

T-0901317 pretreatment improved the vasoconstrictive and vasorelaxation function of the aorta

Vessel contraction response induced by increasing doses of KCl and norepinephrine (NE) was impaired in the AS group compared with the CON group (Fig. 5, $P < 0.05$). LXR agonist pretreatment improved the contractive vessel response to KCl and NE. However, LXR agonist treatment

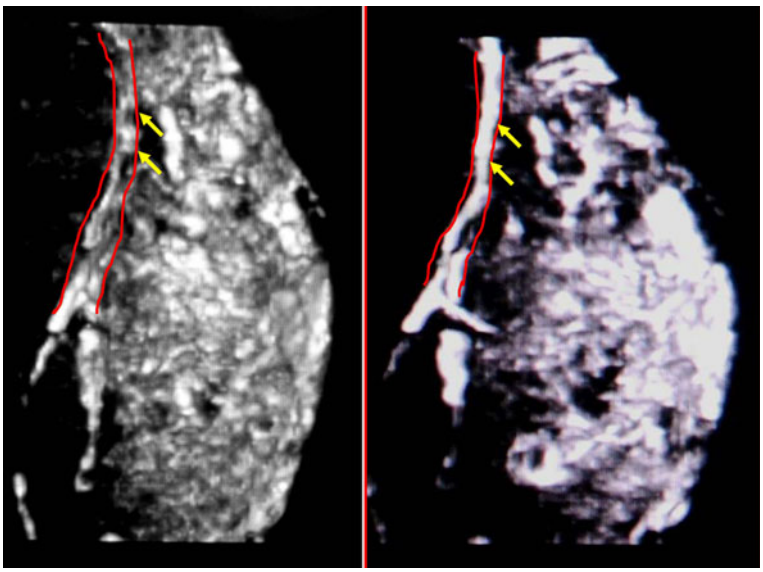

Fig. 2 Effects of T-0901317 on atherosclerotic plaques burden. Representative MRI images of aorta are shown. Diffuse atherosclerotic plaques are indicated in the AS group (**a**). Decreased atherosclerotic plaques burden and clear vessel wall structure are indicated in the AS + LXRa group (**b**)

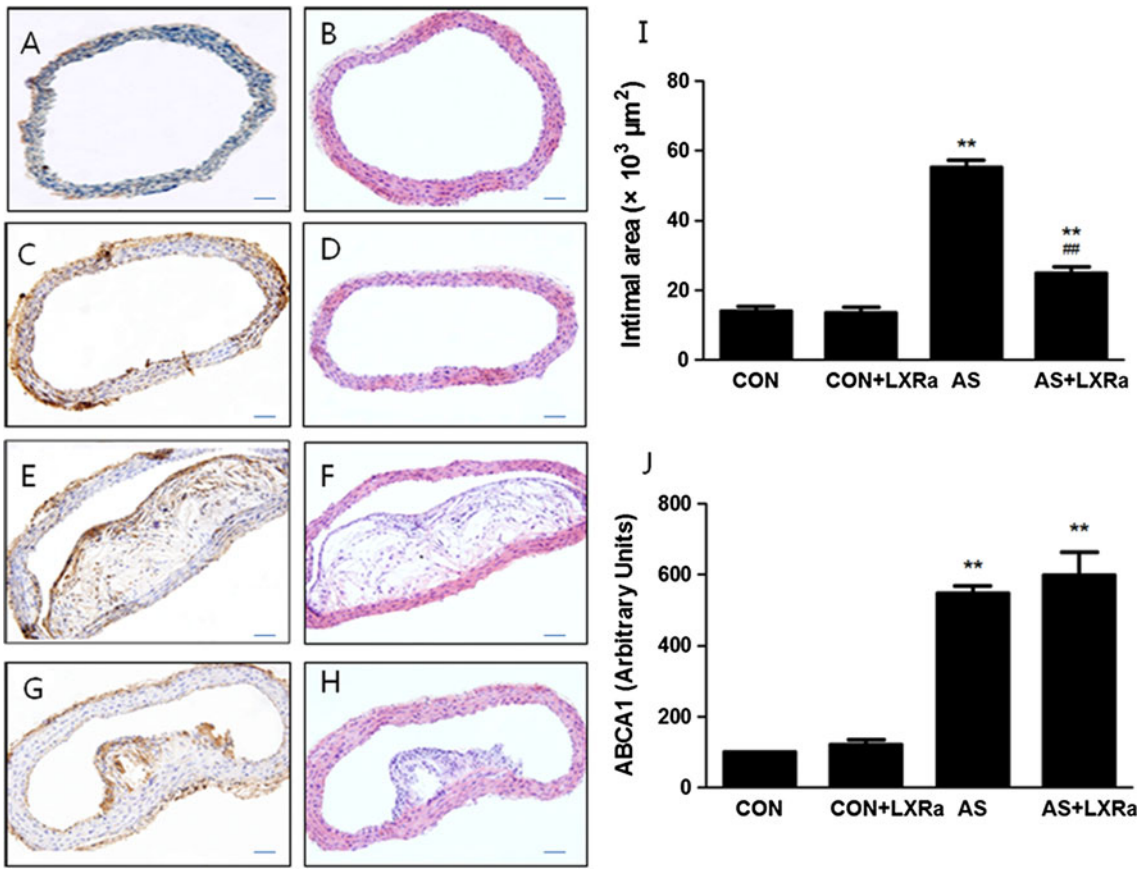

Fig. 3 Effect of T0901317 on atherosclerosis development and ABCA1 expression in aorta. Shown are representative HE staining (**b**, **d**, **f**, **h**) and immunohistochemical staining of ABCA1 (**a**, **c**, **e**, **g**) in cross-sections of aorta. The effects of T0901317 on intimal area (**i**) and effects of T0901317 on ABCA1 expression (**j**) after 6 weeks of treatment. Data represent mean values ± SEM ($n = 4$ mice per group). $^{**}P < 0.05$ vs. CON (control) group, $^{\#\#}P < 0.05$ vs. AS (atherosclerosis) group. Bar = 50 μm

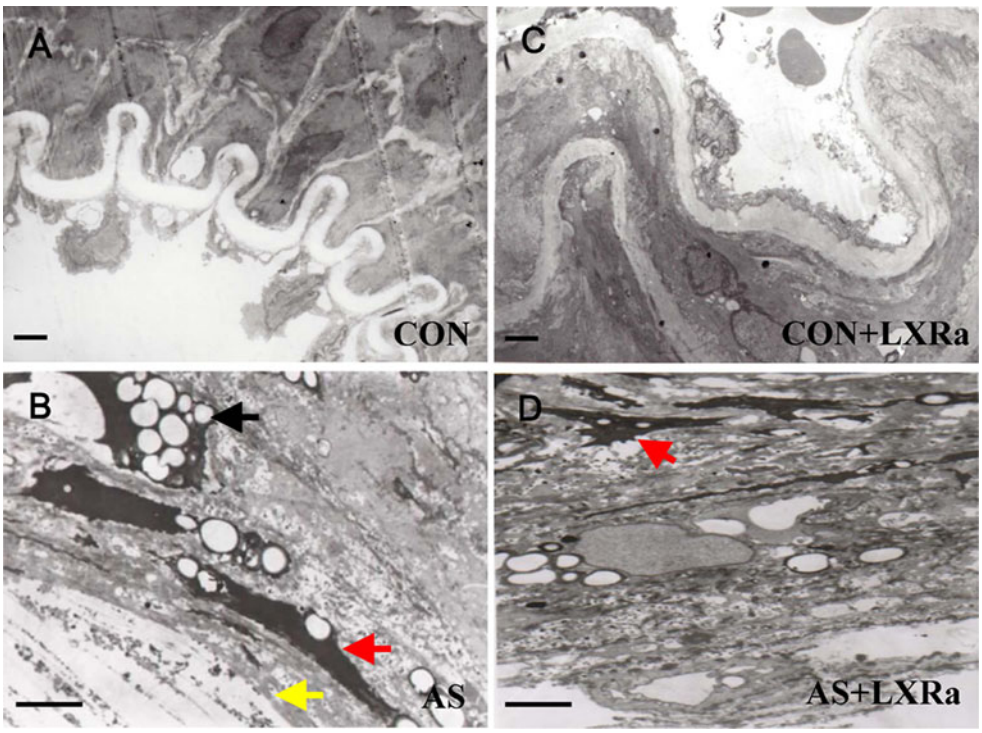

Fig. 4 The ultrastructure changes of mice thoracic aortic tissue as shown by emission electron microscopy. Representative cross-sections of aortic tissue isolated from four treatment groups. Black arrow indicates foam cells. Red arrow indicates migrant smooth muscle cells. Yellow arrow indicates cholesterol crystals. **a** CON group, **b** AS group, **c** AS + LXRa group, **d** CON + LXRa group. Bar = 5 μm

did not restore contraction to the levels observed in the non-atherosclerotic control groups (Fig. 5). There was no significant difference in vessel contraction between the T0901317 treated and untreated non-atherosclerotic groups (i.e. CON vs. CON + LXRa).

We also sought to evaluate the in vitro vasorelaxation response of aortic root sections to acetylcholine (ACh) and sodium nitroprusside (SNP). As expected, vessel dilation in response to ACh was impaired in the AS group compared with the CON group. However, the LXR agonist partially restored the dilative response. Similarly, no significant differences were observed between the CON and CON + LXRa groups. The vessel dilative response induced by SNP was comparable in all four groups (Fig. 5).

We determined the expression of phosphorylated Akt and eNOS in cells treatment with different regimens. The p-eNOS expression was increased by T0901317 treatment by 27.4 %. Cholesterol treatment decreased the p-eNOS expression by about 58.1 %, which was then antagonized by T0901317 treatment ($P < 0.05$). The p-Akt expression showed a similar manner. LY294002 treatment could partly block the upregulating effect of T0901317 on phospho-Akt and phospho-eNOS expression (Fig 6c, d). The changes of eNOS phosphorylation may partly explain the vasomotor function alterations of the aorta.

T-0901317 pretreatment increased the ABCA1 expression in the arterial wall

The aortic tissues were collected from each group at the end of the treatment period and protein content was analyzed by Western blot. The expression of ABCA1 was significantly higher in the AS group than in the CON group (Fig. 6a, $P < 0.05$). LXR agonist pretreatment further increased the ABCA1 protein expression level in the arterial wall compared with the untreated AS group (Fig. 6a, $P < 0.05$). No significant differences between the non-atherosclerotic CON and CON + LXRa groups were observed.

In cell culture studies, the expression of ABCG1 showed a similar manner with ABCA1, which was enhanced by cholesterol stimulation and T0901317. T0901317 plus cholesterol treatment showed a slight tendency toward increase (about 12 %), which was not statistically significant. The PI3 K inhibitor LY294002 did not affect the ABCG1 upregulating effects of T0901317 (Fig 6b).

Discussion

The liver X receptor (LXR) is a member of the nuclear receptor family of transcription factors and is closely

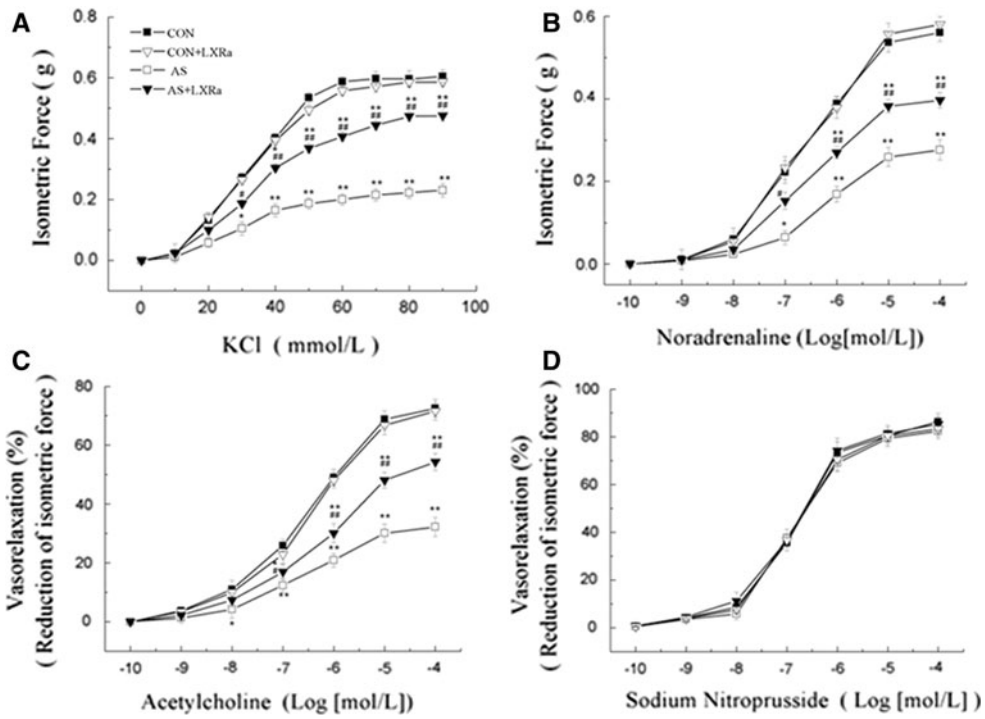

Fig. 5 Vascular ring analysis of the four treatment groups. Shown are cumulative dose–response curves of thoracic aortic ring contraction in response to potassium chloride (**a**), noradrenaline (**b**), acetylcholine (**c**), and sodium nitroprusside (**d**) stimulation. Data represent mean values ± SEM ($n = 4$ mice per group). $^{*}P < 0.05$, $^{**}P < 0.01$ vs. CON (control) group, $^{\#}P < 0.05$, $^{\#\#}P < 0.01$ vs. AS (atherosclerosis) group

related to nuclear receptors such as peroxisome proliferator-activated receptor (PPAR), farnesoid X receptor (FXR) and retinoid X receptor (RXR) [5]. Liver X receptors have been identified as important regulators of cholesterol, fatty acid, and glucose homeostasis [6]. LXRs were previously classified as orphan nuclear receptors. However, upon the discovery of endogenous oxysterols as ligands, they were subsequently recategorized. LXRs have been shown to be involved in a variety of pathophysiological processes, such as cancer [7], Alzheimer's disease [8], diabetes [9], inflammation [10], stroke [11] and stem cell differentiation [12]. In particular, LXR agonists have been implicated in the treatment of atherosclerosis [13, 14].

A study by Joseph et al. has previously shown that chronic administration of GW3965, a synthetic LXR ligand, significantly reduced atherosclerosis in both $LDLR^{-/-}$ mice and $ApoE^{-/-}$ mice [15]. Terasaka et al. found that T-0901317, the LXR ligand used in this study, significantly reduced the atherosclerotic lesions in $LDLR^{-/-}$ mice and increased serum HDL-C levels, without affecting serum total cholesterol levels. These anti-atherogenic effects correlated with the plasma concentration of T-0901317 [4]. Verschuren et al. showed that T0901317 suppressed lesion evolution and promoted lesion regression as assessed by measurement of lesion number, area, and severity [16]. Furthermore, they also demonstrated that T-0901317 could significantly increase plasma triglyceride and total cholesterol levels, suppress endothelial monocyte adhesion, and induce the expression of the cholesterol efflux-related genes apolipoprotein E (ApoE), ATP binding cassette transporters A1 and G1 (ABCA1 and ABCG1). In the present study, we confirmed the anti-atherosclerotic effect of T-0901317 by MRI imaging, immunohistochemical staining and ultrastructural observation using transmission electron microscopy. We investigated the ABCA1 protein expression in the aortic tissue, which showed that T-0901317 significantly increased the expression of ABCA1 in the vascular wall. This upregulation of ABCA1 expression may partly explain the anti-atherosclerotic effect of T-0901317, as ABCA1 is a known promoter of cholesterol efflux from macrophages, smooth muscle cells and endothelial cells in atherosclerotic areas [17]. In addition, foam cell formation and cholesterol crystal deposition were found to be markedly reduced in the T-0901317 treated group.

One concern regarding clinical use of LXR agonists such as GW3965 and T-0901317 for treatment of atherosclerosis is that they may induce hypertriglyceridemia and possibly hepatic steatosis [14]. Indeed, in this study we found increased serum triglyceride levels in the LXRa-treated animals, consistent with previous reports [4]. However, we observed no obvious increase in the extent of liver steatosis in the LXRa-treated groups (data not shown).

The concern about the possible side effect of LXR agonists was further reduced with the development of a new compound N,N-dimethyl-3β-hydroxy-cholenamide (DMHCA). Kratzer et al. recently found that long-term administration of DMHCA over the course of 11 weeks

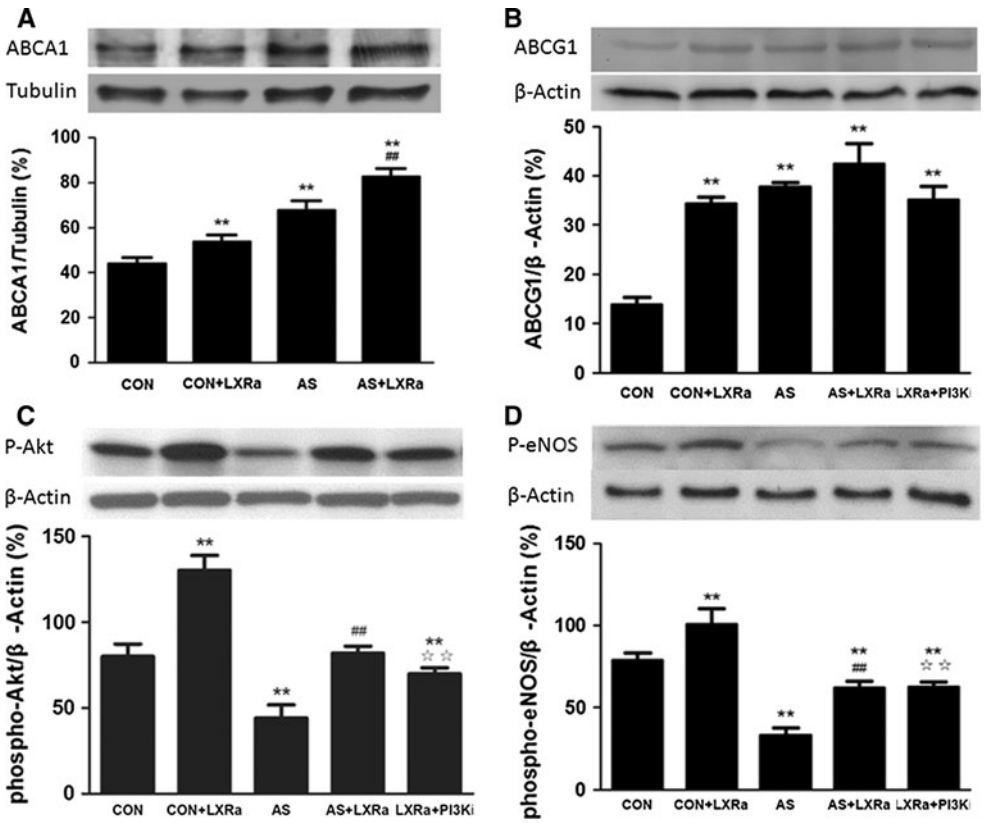

Fig. 6 Western blot analysis. Shown are ABCA1 expression in aortic tissues (**a**) and ABCG1 (**b**), phosphorylated Akt (**c**) and phosphorylated eNOS (**d**) expression in cultured ECs ($n = 4$ mice per group). $^{*}P < 0.05$, $^{**}P < 0.01$ vs. CON (control) group, $^{\#}P < 0.05$, $^{\#\#}P < 0.01$ vs. AS (atherosclerosis) group

significantly reduced lesion formation in male and female ApoE$^{-/-}$ mice [18], and DMHCA did not increase hepatic triglyceride (TG) levels in male or female ApoE$^{-/-}$ mice. Thus, the pro-hypertriglyceridemia effect would not be an obstacle for the application of LXR agonists.

To date, a number of groups have explored the effects of various LXR agonists on the structure of the atherosclerotic plaque. An additional critical determinant in the severity of clinical symptomatology in the context of stenosis is arterial vasorelaxation capability [19, 20]. In this study, besides confirming the anti-atherosclerotic effects of T-0901317, we demonstrated its significant promotion of arterial responsiveness to vasoactive agents such as ACh. We also noticed changes in the endothelial localization of ABCA1 in mice treated with T-0901317. ABCA1 is normally expressed in macrophages [21] and smooth muscle cells, and plays an important role in the process of lipid transport and foam cell formation. Vascular endothelial cells do not undergo foam cell transformation and do not accumulate cholesterol in atherosclerotic plaques to the same extent as macrophages or smooth muscle cells. However, vascular endothelial cells do express receptors for oxidized lipoproteins, undergo receptor-mediated endocytosis of lipoproteins, and carry out the biochemical pathways for sterol synthesis. For instance, Hassan et al. have demonstrated that human umbilical vein endothelial cells (HUVECs) and human aortic endothelial cells (HAECs) express high levels of ABCG1 upon cholesterol stimulation in vitro (which was confirmed by our results) [22], while our ex vivo data using murine aortic samples showed markedly increased ABCA1 expression by the aortic endothelium after cholesterol stimulation, which indicated a self-compensatory mechanism to counteract the high cholesterol intake. Available evidence supports the involvement of both ABCA1 and ABCG1 in endothelial protection [23–27]. For instance, Terasaka et al. showed with an ABCG1$^{-/-}$ mouse model that ABC transporters mediate improved endothelial function in high fat diet fed mice [27]. Similarly, our data indicated that upregulation of ABCA1 may also be involved in the endothelial-protective effect of the LXR agonist T-0901317.

In cell culture studies, we found that cholesterol stimulation decreased the expression of phospho-Akt and phospho-eNOS, while T0901317 increased the expression of phospho-Akt and phospho-eNOS significantly in both the cholesterol treated and untreated setting. The increased bioavailability of nitric oxide that follows may partly explain the vasoactive effects of T0901317.

In summary, the present study showed that the LXR agonist T-0901317 can suppress the progression of atherosclerosis induced by genetic and dietary risk factors by regulating ABCA1 and ABCG1 expression. An important finding is that T-0901317 improves the compliance and endothelium-dependent vasorelaxation of the

atherosclerotic arteries, and the mechanism of this effect may include increased phosphorylation of Akt and eNOS.

Acknowledgments This work was supported by National Nature Science Foundation of China (No. 81090274, No. 81090270, No. 81100579), Innovation Team Start-up Grant by China Department of Education (2010CXTD01) and China's Ministry of Science and Technology 863 Program (2012AA02A603).

Conflict of interest None declared.

References

1. Brooks-Wilson A, Marcil M, Clee SM, Zhang LH, Roomp K, van Dam M, et al. Mutations in ABC1 in Tangier disease and familial high-density lipoprotein deficiency. Nat Genet. 1999;22:336–45.
2. Zhang LN, Zhang LF, Ma J. Simulated microgravity enhances vasoconstrictor responsiveness of rat basilar artery. J Appl Physiol. 2001;90:2296–305.
3. Sangha DS, Vaziri ND, Ding Y, Purdy RE. Vascular hyporesponsiveness in simulated microgravity: role of nitric oxide-dependent mechanisms. J Appl Physiol. 2000;88:507–17.
4. Terasaka N, Hiroshima A, Koieyama T, Ubukata N, Morikawa Y, Nakai D, et al. T-0901317, a synthetic liver X receptor ligand, inhibits development of atherosclerosis in LDL receptor-deficient mice. FEBS Lett. 2003;536:6–11.
5. Willy PJ, Umesono K, Ong ES, Evans RM, Heyman RA, Mangelsdorf DJ. LXR, a nuclear receptor that defines a distinct retinoid response pathway. Genes Dev. 1995;9:1033–45.
6. Schultz JR, Tu H, Luk A, Repa JJ, Medina JC, Li L, et al. Role of LXRs in control of lipogenesis. Genes Dev. 2000;14:2831–8.
7. Fukuchi J, Kokontis JM, Hiipakka RA, Chuu CP, Liao S. Antiproliferative effect of liver X receptor agonists on LNCaP human prostate cancer cells. Cancer Res. 2004;64:7686–9.
8. Koldamova RP, Lefterov IM, Staufenbiel M, Wolfe D, Huang S, Glorioso JC, et al. The liver X receptor ligand T0901317 decreases amyloid beta production in vitro and in a mouse model of Alzheimer's disease. J Biol Chem. 2005;280:4079–88.
9. Basciano H, Miller A, Baker C, Naples M, Adeli K. LXRalpha activation perturbs hepatic insulin signaling and stimulates production of apolipoprotein B-containing lipoproteins. Am J Physiol Gastrointest Liver Physiol. 2009;297:G323–32.
10. Joseph SB, Castrillo A, Laffitte BA, Mangelsdorf DJ, Tontonoz P. Reciprocal regulation of inflammation and lipid metabolism by liver X receptors. Nat Med. 2003;9:213–9.
11. Chen J, Cui X, Zacharek A, Roberts C, Chopp M. eNOS mediates TO90317 treatment-induced angiogenesis and functional outcome after stroke in mice. Stroke: A Journal of Cerebral Circulation. 2009;40:2532–8.
12. Jeong Y, Mangelsdorf DJ. Nuclear receptor regulation of stemness and stem cell differentiation. Exp Mol Med. 2009;41:525–37.
13. Song C, Hiipakka RA, Liao S. Auto-oxidized cholesterol sulfates are antagonistic ligands of liver X receptors: implications for the development and treatment of atherosclerosis. Steroids. 2001;66:473–9.
14. Bennett DJ, Cooke AJ, Edwards AS. Non-steroidal LXR agonists; an emerging therapeutic strategy for the treatment of atherosclerosis. Recent Pat Cardiovasc Drug Discov. 2006;1:21–46.
15. Joseph SB, McKilligin E, Pei L, Watson MA, Collins AR, Laffitte BA, et al. Synthetic LXR ligand inhibits the development of atherosclerosis in mice. Proc Natl Acad Sci USA. 2002;99:7604–9.
16. Verschuren L, de Vries-van der Weij J, Zadelaar S, Kleemann R, Kooistra T. LXR agonist suppresses atherosclerotic lesion growth and promotes lesion regression in apoE*3Leiden mice: time course and mechanisms. J Lipid Res. 2009;50:301–11.
17. de la Llera-Moya M, Drazul-Schrader D, Asztalos BF, Cuchel M, Rader DJ, Rothblat GH. The ability to promote efflux via ABCA1 determines the capacity of serum specimens with similar high-density lipoprotein cholesterol to remove cholesterol from macrophages. Arterioscler Thromb Vasc Biol. 2010;30:796–801.
18. Kratzer A, Buchebner M, Pfeifer T, Becker TM, Uray G, Miyazaki M, et al. Synthetic LXR agonist attenuates plaque formation in apoE-/- mice without inducing liver steatosis and hypertriglyceridemia. J Lipid Res. 2009;50:312–26.
19. Johnstone MT, Creager SJ, Scales KM, Cusco JA, Lee BK, Creager MA. Impaired endothelium-dependent vasodilation in patients with insulin-dependent diabetes mellitus. Circulation. 1993;88:2510–6.
20. Hamabe A, Takase B, Uehata A, Kurita A, Ohsuzu F, Tamai S. Impaired endothelium-dependent vasodilation in the brachial artery in variant angina pectoris and the effect of intravenous administration of vitamin C. Am J Cardiol. 2001;87:1154–9.
21. Schmitz G, Kaminski WE, Porsch-Ozcurumez M, Klucken J, Orso E, Bodzioch M, et al. ATP-binding cassette transporter A1 (ABCA1) in macrophages: a dual function in inflammation and lipid metabolism? Pathobiology. 1999;67:236–40.
22. Hassan HH, Denis M, Krimbou L, Marcil M, Genest J. Cellular cholesterol homeostasis in vascular endothelial cells. Can J Cardiol. 2006;22(Suppl B):35B–40B.
23. Jaccard E, Widmann C. ABC transporters: hDL-regulated gatekeepers at the endothelial border. Curr Opin Lipidol. 2009;20:526–7.
24. Curtiss LK, Valenta DT, Hime NJ, Rye KA. What is so special about apolipoprotein AI in reverse cholesterol transport? Arterioscler Thromb Vasc Biol. 2006;26:12–9.
25. Rohrer L, Ohnsorg PM, Lehner M, Landolt F, Rinninger F, von Eckardstein A. High-density lipoprotein transport through aortic endothelial cells involves scavenger receptor BI and ATP-binding cassette transporter G1. Circ Res. 2009;104:1142–50.
26. Cavelier C, Rohrer L, von Eckardstein A. ATP-Binding cassette transporter A1 modulates apolipoprotein A-I transcytosis through aortic endothelial cells. Circ Res. 2006;99:1060–6.
27. Terasaka N, Yu S, Yvan-Charvet L, Wang N, Mzhavia N, Langlois R, et al. ABCG1 and HDL protect against endothelial dysfunction in mice fed a high-cholesterol diet. J Clin Invest. 2008;118:3701–13.